AIP | Applied Physics Letters

Monolithic polymer microlens arrays with antireflective nanostructures

Hyukjin Jung and Ki-Hun Jeong

Citation: Applied Physics Letters **101**, 203102 (2012); doi: 10.1063/1.4747717
View online: http://dx.doi.org/10.1063/1.4747717
View Table of Contents: http://scitation.aip.org/content/aip/journal/apl/101/20?ver=pdfcov
Published by the AIP Publishing

Over **700** papers & presentations on multiphysics simulation VIEW NOW ▸

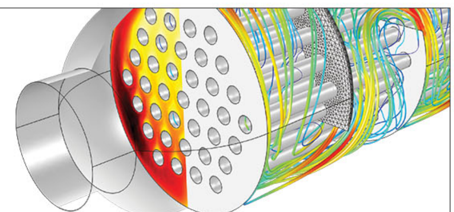

This article is copyrighted as indicated in the article. Reuse of AIP content is subject to the terms at: http://scitation.aip.org/termsconditions. Downloaded to IP: 143.248.118.126 On: Thu, 05 Dec 2013 02:39:25

Monolithic polymer microlens arrays with antireflective nanostructures

Hyukjin Jung and Ki-Hun Jeong[a)]
Department of Bio and Brain Engineering, KAIST Institute for Optical Science and Technology, Korea Advanced Institute of Science and Technology (KAIST), 291 Daehak-ro, Yuseong-gu, Daejeon 305-701, South Korea

(Received 25 April 2012; accepted 8 August 2012; published online 12 November 2012)

This work reports a novel method for fabricating monolithic polymer microlens arrays with antireflective nanostructures (AR-MLAs) at wafer level. The antireflective nanostructures (ARS) were fabricated by etching the curved surface of polymer microlens with a metal annealed nanoisland mask. The effective refractive index of ARS was controlled with the etch profile of nanostructures to reduce the mismatch in refractive indices at air-lens interface. The reflectance of AR-MLAs decreases below 4% from 490 nm to 630 nm in wavelength. The lens transmission significantly increases by 67% across the visible spectrum by minimizing the reflection and absorption, compared to that of MLAs without ARS. © *2012 American Institute of Physics*.
[http://dx.doi.org/10.1063/1.4747717]

Monolithic polymer microlens arrays (MLAs) provide substantial benefits in improving photon collection onto image sensor arrays (ISA) such as charge-coupled device (CCD) or complementary metal–oxide–semiconductor (CMOS). Among many different methods for monolithic fabrication of refractive polymer MLAs, resist-melting, i.e., the reflow of polymer cylindrical micropatterns over the glass transition temperature to form the lenslet shape by the surface energy minimization, has been widely used in industrial applications due to the facility of direct integration, large area fabrication, and precise alignment with ISA.[1,2] However, transmission efficiency of polymer MLAs is still limited by high reflection from a lens surface due to the optical index mismatch at the air-lens interface and high absorption of lens polymer in the visible spectrum. The lens reflection can be commonly reduced by coating either a single layer of low-index material below water or alternating layers of contrasting refractive index. Both methods are still not affordable for directly applying to monolithic polymer MLAs on ISA due to lack of solid materials with low refractive index or multiple fabrication steps.[3] Besides, high performance of anti-reflection with low absorption is not secured across the entire visible spectrum.

Nature offers antireflection in a dissimilar fashion. Compound eyes found in an insect such as a Morpho butterfly (*Morpho didius*) consist of honeycomb-packed hexagonal corneal lenses like MLAs. Each corneal lens surface is covered with nanonipples at sub-wavelength scale of visible light as shown in Fig. 1(a). The nanonipples serve as antireflective nanostructures (ARS) over the visible spectrum by providing a low index layer to effectively reduce the Fresnel reflection due to the optical index mismatch at air-lens interface.[4–8] For the last decade, the diverse methods of ARS fabrication have been extensively applied in a biomimetic fashion on planar substrates such as silicon,[9,10] III–V semiconductor,[11,12] glass,[13,14] or polymer.[15] More recently, the ARS over the curved surface of MLAs have been employed by using an anodic aluminum oxide (AAO) based nanoimprint stamp[16] or a laser interference lithography.[17,18] However, all the previous methods still have many technical difficulties in implementing ARS over MLAs with low cost, large area fabrication, and direct ISA integration with precise alignment.

This work presents the nanofabrication method and the optical characterizations of monolithic polymer microlens arrays with antireflective nanostructures (AR-MLAs) at wafer level. While conventional MLAs (top) have high reflection from smooth polymer surface, AR-MLAs (bottom) significantly reduce the lens reflection by matching the optical index at air-lens surface as shown in Fig. 1(b). The monolithic fabrication of AR-MLAs was done by incorporating a silver annealed nanoisland mask and isotropic dry etching the lens surfaces as illustrated in Fig. 2(a). Polymer MLAs were prepared on a 4-in. soda-lime glass wafer by using a conventional resist melting method. A positive tone photoresist (AZ 1512, AZ Electronic Materials) was initially defined with cylindrical micropatterns by using photolithography.

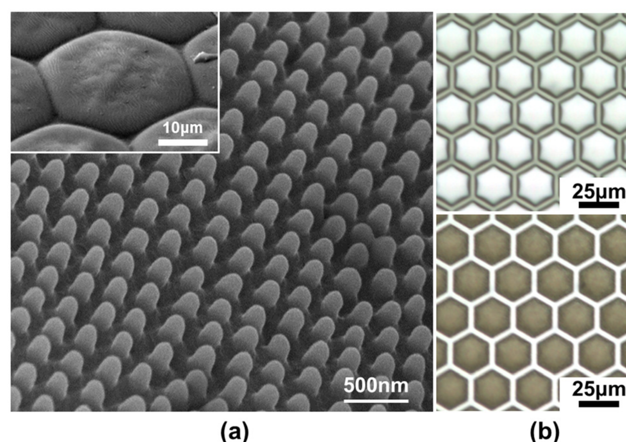

FIG. 1. ARS over monolithic polymer microlens arrays. (a) SEM images of nanonipples as antireflective nanostructures on a hexagonal corneal lens (inset panel) of a Morpho butterfly eye (*M. didius*). (b) Reflection microscopic images of polymer microlens arrays without (top) and with (bottom) antireflective nanostructures on a glass wafer.

a)Author to whom correspondence should be addressed. Electronic mail: kjeong@kaist.ac.kr.

 © 2012 American Institute of Physics

This article is copyrighted as indicated in the article. Reuse of AIP content is subject to the terms at: http://scitation.aip.org/termsconditions. Downloaded to IP: 143.248.118.126 On: Thu, 05 Dec 2013 02:39:25

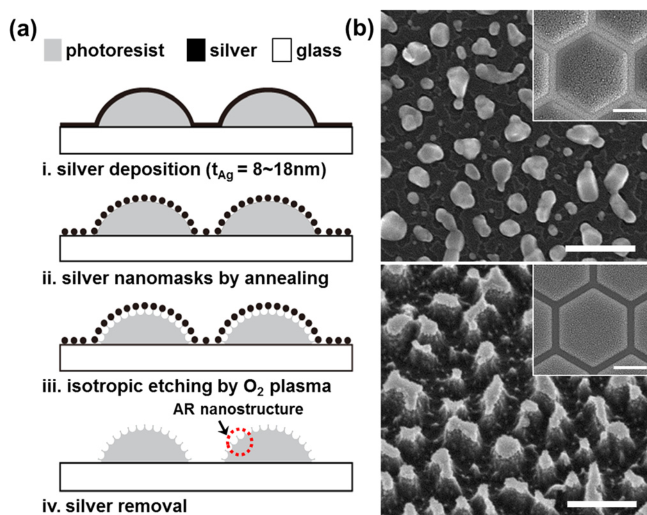

FIG. 2. Monolithic nanofabrication of polymer AR-MLAs at wafer level. (a) Nano- and microfabrication procedures of polymer AR-MLAs by using a silver annealed nanoisland mask and an isotropic dry etching. (b) SEM images of polymer microlens surface covered with silver annealed nanoislands (top) and after dry etching and silver removal (bottom). Scale bar: (both panels) 500 nm; (inset panels) 10 μm.

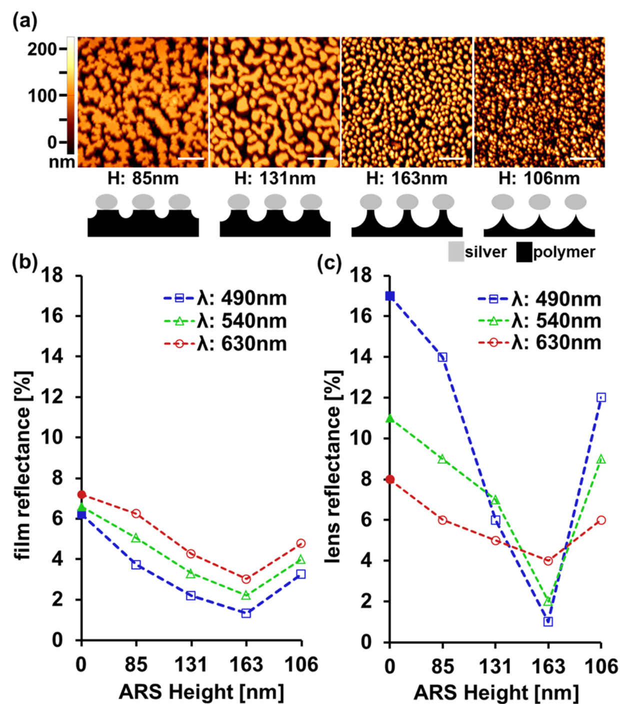

FIG. 3. Lens reflectance from AR-MLAs depending on different shapes of antireflective nanostructures. (a) AFM images of the diverse shapes of antireflective nanostructures after the removal of silver nanoislands as the isotropic etching time increases (scale bar: 1 μm). (b) Spectral reflectance of antireflective nanostructures on a planar polymer surface (0 ARS height indicates planar polymer surface without ARS). (c) Spectral reflectance of antireflective nanostructures on the curved surfaces of polymer microlens arrays: The minimum reflectance of AR-MLAs is comparable to that of ARS on a planar surface across the full visible spectrum (0 ARS height indicates smooth lens surface without ARS).

The micropattern arrays were then reflowed and hardened by thermal cross-linking at 180 °C for 30 min in a convection oven. Antireflective nanostructures were directly fabricated over the curved surface of MLAs by using isotropic etching with a silver annealed nanoisland mask. First, a thin silver film in Volmer-Weber mode was directly deposited on the MLAs by thermal evaporation.[19] The thin silver film was then transformed into silver nanoislands by using thermal dewetting on a hot plate at 240 °C for 1 h in ambient condition. The initial silver thickness of 8 to 18 nm effectively forms nanoislands with moderate uniformity without either degrading or further remelting the cross-linked lens polymer. The size and gap of nanoislands can be statistically controlled by the initial thickness of silver film. For example, the average pitch increases from 90 nm to 310 nm as the silver film increases from 8 to 18 nm in thickness. However, the formation of silver nanoislands during thermal dewetting at such low temperature was not observed over 25 nm in thickness. Next, the polymer lens surface was isotropically etched with the silver nanoisland mask by using oxygen plasma (RF power of 150 W, oxygen gas of 50 sccm, argon gas of 50 sccm, and chamber pressure of 270 mTorr), where each silver nanoisland efficiently protects the underneath polymer with high etch selectivity. Finally, the silver nanoislands were selectively removed with a wet etchant (Silver Etchant TFS, Transene Company, Inc.) without any damage of the polymer MLAs. Fig. 2(b) shows the SEM images of a silver annealed nanoisland mask (initial silver thickness: 18 nm) and antireflective nanostructures over the MLA surfaces.

The lens reflectance was first measured with AR-MLAs depending on the shapes of antireflective nanostructures. Different etch profiles of ARS on polymer MLA surfaces were achieved as shown in the AFM images of Fig. 3(a). The spectral reflectance of antireflective nanostructures on a planar polymer surface was measured by using a microscopic spectrometer (MicroSpec-2300i, Princeton Instruments) over a range of 490 nm to 630 nm in wavelength as shown in Fig. 3(b). The measured results show the reflectance decreases in the visible spectrum as the height of nanostructures increases (H = 85 nm, 131 nm, and 163 nm) because the effective index of refraction at air-lens interface decreases with the isotropic etching time. On the contrary, excessive isotropic etching causes the aerial reduction of polymer nanostructures (H = 106 nm), which results in the increase of reflectance due to increase of effective refractive index over the MLA surfaces. The result also demonstrates that the spectral reflectance slightly decreases as the nanostructure height increases. The reflectance of ARS on a planar surface exhibits 1.3% at 490 nm and 3.8% at 630 nm, while that of a smooth polymer surface is 6.3% at 490 nm and 7.2% at 630 nm in wavelength. Most photosensitive polymers with positive tone typically show high absorption near ultraviolet wavelengths due to the existence of photosensitive molecules.[20] The low reflectance at 490 nm mainly results from high absorption of ARS because the absorption coefficient of lens polymer increases as the wavelength becomes shorter (see the absorption coefficient of AZ-1512 shown in the supplementary material in Fig. S1).[24] The reflectance from ARS on the lens surfaces of MLAs can be calculated from the measured transmittance and the absorptance of MLAs with a packing density as shown in Fig. 3(c). The transmittance of MLAs was measured by using an integrating sphere with a spectrophotometer (SM642, Spectral Products), where a white light LED with a slight divergence angle of 6.89° was

This article is copyrighted as indicated in the article. Reuse of AIP content is subject to the terms at: http://scitation.aip.org/termsconditions. Downloaded to IP: 143.248.118.126 On: Thu, 05 Dec 2013 02:39:25

illuminated on the lens surfaces of MLAs (see the measured transmittance shown in the supplementary material in Fig. S2).[24] Note that the spectral power of transmitted light was attenuated by both the absorption and the reflection arising from MLAs. First, the absorptance, i.e., the fraction of light absorbed by MLAs to the incident light power, was calculated from the absorption coefficient, the optical path length, and the packing density of hexagonal MLAs. The measured absorption coefficients of the lens polymer are 0.266 μm^{-1} at 490 nm and 0.004 μm^{-1} at 630 nm in wavelength (M2000D, Woollam Company, Inc.). The packing densities are 0.70 for normal MLAs with a hexagonal arrangement and 0.68 for AR-MLAs (H = 163 nm). Small variance in the packing density and the optical path length of MLAs results from the isotropic removal of absorbing volume during the polymer etching for ARS formation, which reduces 3% at 490 nm and 1% at 630 nm in the absorptance of AR-MLAs (H = 163 nm). The lens reflectance of MLAs was then calculated by one minus the sum of the transmittance and the absorptance of MLAs as shown in Fig. 3(c). The results show that the reflectance of normal MLAs substantially increases due to the curved geometry and rough edges of the lens, compared to that of the planar surface. However, the reflectance of AR-MLAs decreases as the height of nanostructures (H = 85 nm, 131 nm, and 163 nm) increases. The minimum reflectance of the curved surfaces of AR-MLAs is comparable to that of ARS on planar surface across the full visible spectrum.

The lens transmission was also measured with AR-MLAs depending on the shapes of antireflective nanostructures. The lens performance of AR-MLAs was characterized with a transmission confocal laser scanning microscope (CLSM) by sequentially imaging the optical sections along the focusing beam under a collimated laser beam at 488 nm. As shown in Fig. 4(a), the optical section in x-z plane shows the focal lengths of AR-MLAs remain constant after the nanofabrication of ARS. The CLSM (LSM510, Carl Zeiss GmbH) image in x-y plane also indicates excellent spatial uniformity of beam spots at the foci of AR-MLAs. The point spread function (PSF) was also extracted from the beam spot of each microlens with different shapes of ARS. The PSFs clearly demonstrate high transmission through AR-MLAs due to the reduction in both reflection and absorption of the microlens. The beam spot sizes of AR-MLAs also remain constant at 1.9 μm full width at half maximum. It turns out that the antireflective nanostructures on MLAs were fabricated without any sacrifice of microlens performance. Fig. 4(b) shows the bright-field projection images of a transparent character "F" captured by both normal MLAs (lower) and AR-MLAs (upper). The intensity distributions along line x-x′ of the captured image of character "F" were also compared for the different shapes of antireflective nanostructures. The results clearly demonstrate that AR-MLAs increase the imaging brightness by 67% across the full visible spectrum due to the significant reduction in lens reflection and absorption.

In summary, this work demonstrates a simple and effective method for directly employing antireflective nanostructures on the curved surface of monolithic polymer microlens arrays over a 4-in. wafer by using metal annealing and isotropic etching. The effective refractive index of antireflective nanostructures was statistically controlled by the etch profile of the curved surface of polymer microlenses to minimize the mismatch in refractive indices at air-polymer interface. The AR-MLAs exhibit light transmittance enhancement over 67% with high uniformity due to the significant reduction in both reflectance and absorptance over a broad range of the visible spectrum. This simple and inexpensive method can provide great potentials for diverse MLA applications such as high sensitive imaging system,[21] solar cells,[22] and projection lithography.[23]

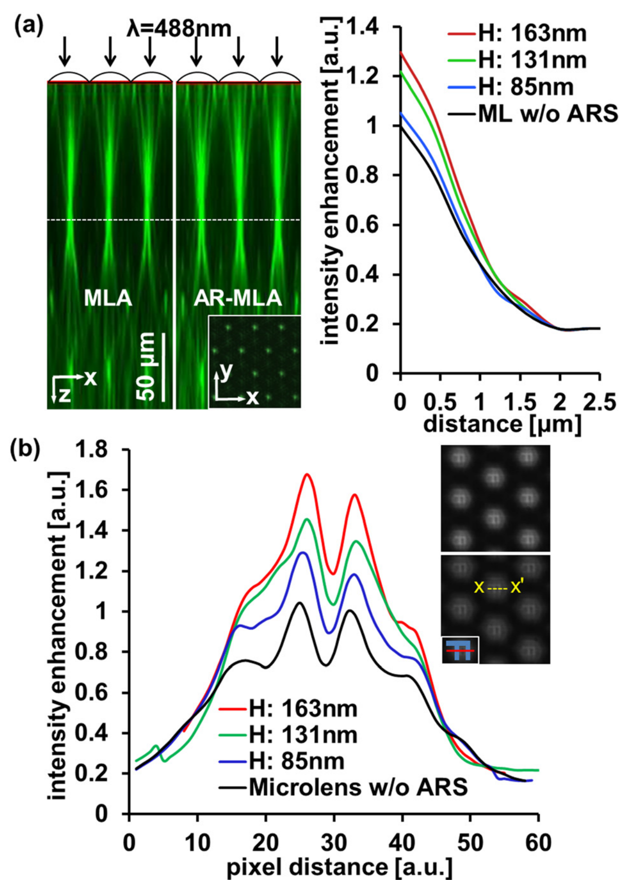

FIG. 4. Lens transmission through conventional MLAs and AR-MLAs depending on the shapes of antireflective nanostructures. (a) 3D optical sectioning of coupled light ($\lambda = 488$ nm) and PSFs at focal planes between MLAs and AR-MLAs by using a modified confocal laser scanning microscopy. (b) Projected image arrays of character "F" captured by AR-MLAs and intensity distribution normalized along line x-x′ from the image under white light illumination.

This work is supported by the National Research Foundation of Korea (NRF) grant funded by the Korea government (MEST) (20120006653, 20120005641, 2011-0031868).

[1]Z. D. Popovic, R. A. Sprague, and G. A. N. Connell, Appl. Opt. **27**(7), 1281–1284 (1988).
[2]R. Volkel, M. Eisner, and K. J. Weible, Microelectron. Eng. **67–68**, 461–472 (2003).
[3]J. Q. Xi, M. F. Schubert, J. K. Kim, E. F. Schubert, M. Chen, S.-Y. Lin, W. Liu, and J. A. Smart, Nature Photon. **1**(3), 176 (2007).
[4]W. H. Miller, G. D. Bernard, and J. L. Allen, Science **162**(3855), 760–767 (1968).
[5]P. B. Clapham and M. C. Hutley, Nature **244**(5414), 281–282 (1973).
[6]P. Vukusic and J. R. Sambles, Nature **424**(6950), 852–855 (2003).
[7]D. G. Stavenga, S. Foletti, G. Palasantzas, and K. Arikawa, Proc. R. Soc. London, Ser. B **273**(1587), 661–667 (2006).

This article is copyrighted as indicated in the article. Reuse of AIP content is subject to the terms at: http://scitation.aip.org/termsconditions. Downloaded to IP: 143.248.118.126 On: Thu, 05 Dec 2013 02:39:25

[8]A. R. Parker and H. E. Townley, Nat. Nanotechnol. **2**(6), 347–353 (2007).
[9]Y.-F. Huang, S. Chattopadhyay, Y.-J. Jen, C.-Y. Peng, T.-A. Liu, Y.-K. Hsu, C.-L. Pan, H.-C. Lo, C.-H. Hsu, Y.-H. Chang, C.-S. Lee, K.-H. Chen, and L.-C. Chen, Nat. Nanotechnol. **2**(12), 770–774 (2007).
[10]Y.-M. Chang, J. Shieh, and J.-Y. Juang, J. Phys. Chem. C **115**(18), 8983–8987 (2011).
[11]S. L. Diedenhofen, G. Vecchi, R. E. Algra, A. Hartsuiker, O. L. Muskens, G. Immink, E. P. A. M. Bakkers, W. L. Vos, and J. G. Rivas, Adv. Mater. **21**(9), 973–978 (2009).
[12]Y. M. Song, E. S. Choi, G. C. Park, C. Y. Park, S. J. Jang, and Y. T. Lee, Appl. Phys. Lett. **97**(9), 093110 (2010).
[13]W. L. Min, B. Jiang, and P. Jiang, Adv. Mater. **20**(20), 3914–3918 (2008).
[14]Y. Li, J. Zhang, S. Zhu, H. Dong, F. Jia, Z. Wang, Z. Sun, L. Zhang, H. Li, W. Xu, and B. Yang, Adv. Mater. **21**(46), 4731–4734 (2009).
[15]K. Choi, S. H. Park, Y. M. Song, Y. T. Lee, C. K. Hwangbo, H. Yang, and H. S. Lee, Adv. Mater. **22**(33), 3713–3718 (2010).
[16]T. Yanagishita, K. Nishio, and H. Masuda, Appl. Phys. Express **2**(2), 022001 (2009).
[17]B. Päivänranta, P.-Y. Baroni, T. Scharf, W. Nakagawa, M. Kuittinen, and H. P. Herzig, Microelectron. Eng. **85**(5–6), 1089–1091 (2008).
[18]A. Mizutani, S. Takahira, and H. Kikuta, Appl. Opt. **49**(32), 6268–6275 (2010).
[19]C. T. Campbell, Surf. Sci. Rep. **27**(1–3), 1–111 (1997).
[20]N. Nordman and O. Nordman, Opt. Eng. **40**(11), 2572–2576 (2001).
[21]R. P. J. Barretto, B. Messerschmidt, and M. J. Schnitzer, Nat. Methods **6**(7), 511 (2009).
[22]K. Tvingstedt, S. Dal Zilio, O. Ingan, and M. Tormen, Opt. Express **16**(26), 21608 (2008).
[23]M. H. Wu and G. M. Whitesides, Adv. Mater. **14**(20), 1502 (2002).
[24]See supplementary material at http://dx.doi.org/10.1063/1.4747717 for the absorption coefficient of AZ-1512 and the measured transmittance of MLAs.

This article is copyrighted as indicated in the article. Reuse of AIP content is subject to the terms at: http://scitation.aip.org/termsconditions. Downloaded to IP: 143.248.118.126 On: Thu, 05 Dec 2013 02:39:25